



Corrections to: “Accurate computation of gravitational field of a tesseroid” by Fukushima (2018) in J. Geod. 92(12):1371–1386

Xiao-Le Deng¹

Received: 15 February 2022 / Accepted: 2 October 2022 / Published online: 19 January 2023
© The Author(s) 2023

Abstract

An accurate method with conditional split, double exponential quadrature rule, and numerical differentiation has been proposed in the paper “Accurate computation of gravitational field of a tesseroid” (Fukushima in J Geod 92(12):1371–1386, <https://doi.org/10.1007/s00190-018-1126-2>, 2018) to compute the gravitational field (i.e. gravitational potential, gravitational acceleration vector, and gravity gradient tensor) of a tesseroid. This study presents the corrections for some formulas in the main paper and electronic supplementary material of Fukushima (J Geod 92(12):1371–1386, <https://doi.org/10.1007/s00190-018-1126-2>, 2018). Moreover, the FORTRAN subroutines `gtess` (or `qgtess`) and `ggtess` (or `qggtess`) in the original codes `xtess.txt` (or `xqgtess.txt`) in double (or quadrature) precision provided by Fukushima (J Geod 92(12):1371–1386, <https://doi.org/10.1007/s00190-018-1126-2>, 2018) are revised. The revised parts have impacts on the calculation of these components of the gravitational acceleration vector (g_ϕ and g_Λ) and gravity gradient tensor ($\Gamma_{\phi\phi}$, $\Gamma_{\phi\Lambda}$, $\Gamma_{\phi H}$, $\Gamma_{\Lambda\Lambda}$, $\Gamma_{\Lambda H}$, and Γ_{HH}). The revised FORTRAN codes `xtess.f90` and `xqgtess.f90` in double and quadrature precision are presented at the GitHub website <https://github.com/xiaoledeng/xtess-xqgtess>. These revised FORTRAN codes can accurately compute the gravitational field of a tesseroid in double and quadrature precision no matter the computation point is located outside, near the surface of, on the surface of, or inside the tesseroid. They can be applied to calculate the gravitational field of the different layers (e.g. atmosphere, topography, crust, and mantle) of the Earth or other celestial bodies, which helps investigate the various geoscience applications, e.g. geoid determination in geodesy and gravity interpretation in geophysics.

Keywords Gravitational field · Numerical differentiation · Numerical integration · Split quadrature · Tesseroid

1 Introduction

In the paper “Accurate computation of gravitational field of a tesseroid” (Fukushima 2018), an accurate method with conditional split, double exponential quadrature rule, and numerical differentiation has been presented for calculating the gravitational potential, gravitational acceleration vector, and gravity gradient tensor of a tesseroid, whereas the expressions for the $\Gamma_{\phi\Lambda}$ and $\Gamma_{\Lambda H}$ components of the gravity gradient tensor in Fukushima (2018) contain formal errors and need to be corrected. Meanwhile, some typos of the negative sign need to be corrected. The two FORTRAN codes `xtess.txt` and `xqgtess.txt` provided by Fukushima (2018) to calculate the gravitational acceleration vector and

gravity gradient tensor of a tesseroid need to be revised in double and quadruple precision.

This study presents the corrections for some formulas and two FORTRAN codes in Fukushima (2018). Furthermore, a numerical experiment is performed to reveal the consequences of the modified formulas and FORTRAN codes.

This study is organized as follows. Sections 2 and 3 present the corrections to some formulas and FORTRAN codes in Fukushima (2018), respectively. The corrected formulas and FORTRAN codes are numerically investigated against analytical solutions for a spherical shell in Sect. 4. Section 5 offers the revised FORTRAN codes `xtess.f90` and `xqgtess.f90`. Conclusions and consequences for Fukushima (2018) are summarized in Sect. 6.

✉ Xiao-Le Deng
xiaole.deng@gis.uni-stuttgart.de; xldeng@whu.edu.cn

¹ Institute of Geodesy, University of Stuttgart, Stuttgart 70174, Germany

2 Corrections to some formulas in Fukushima (2018)

Regarding the expressions of the diagonal component $(\partial^2 V / \partial H^2)_{\Phi, \Lambda}$ of the second-order partial derivatives in Fukushima (2018), the $+\frac{(\Delta_2 H)^2}{12} \left(\frac{\partial^4 V}{\partial H^4}\right)$ term in Eq. (25) should be replaced by $-\frac{(\Delta_2 H)^2}{12} \left(\frac{\partial^4 V}{\partial H^4}\right)$, where the sign is wrong, and it is a typo. Equation (25) should be changed to:

$$\begin{aligned} & \left(\frac{\partial^2 V}{\partial H^2}\right)_{\Phi, \Lambda} \\ &= \frac{V(\Phi, \Lambda, H + \Delta_2 H) - 2V(\Phi, \Lambda, H) + V(\Phi, \Lambda, H - \Delta_2 H)}{(\Delta_2 H)^2} \\ &= -\frac{(\Delta_2 H)^2}{12} \left(\frac{\partial^4 V}{\partial H^4}\right) - \frac{(\Delta_2 H)^4}{360} \left(\frac{\partial^6 V}{\partial H^6}\right) - \dots \quad (1) \end{aligned}$$

Similarly, for the expressions of the non-diagonal component $[\partial^2 V / (\partial \Phi \partial \Lambda)]_H$ of the second-order partial derivatives in Eq. (26) of Fukushima (2018), the $+\frac{(\Delta_2 \Phi)(\Delta_2 \Lambda)}{36} \left(\frac{\partial^4 V}{\partial \Phi^2 \partial \Lambda^2}\right)$ term is wrong. It should be replaced by the $-\frac{(\Delta_2 \Phi)^2(\Delta_2 \Lambda)^2}{36} \left(\frac{\partial^6 V}{\partial \Phi^3 \partial \Lambda^3}\right)$, and it is a typo. Meanwhile, two terms $-\frac{(\Delta_2 \Phi)^2}{6} \left(\frac{\partial^4 V}{\partial \Phi^3 \partial \Lambda}\right)$ and $-\frac{(\Delta_2 \Lambda)^2}{6} \left(\frac{\partial^4 V}{\partial \Phi \partial \Lambda^3}\right)$ are missing. Equation (26) should be changed to:

$$\begin{aligned} & \left(\frac{\partial^2 V}{\partial \Phi \partial \Lambda}\right)_H = [V(\Phi + \Delta_2 \Phi, \Lambda + \Delta_2 \Lambda, H) \\ & - V(\Phi + \Delta_2 \Phi, \Lambda - \Delta_2 \Lambda, H) \\ & - V(\Phi - \Delta_2 \Phi, \Lambda + \Delta_2 \Lambda, H) \\ & + V(\Phi - \Delta_2 \Phi, \Lambda - \Delta_2 \Lambda, H)] / [4(\Delta_2 \Phi)(\Delta_2 \Lambda)] \quad (2) \\ & - \frac{(\Delta_2 \Phi)^2}{6} \left(\frac{\partial^4 V}{\partial \Phi^3 \partial \Lambda}\right) - \frac{(\Delta_2 \Lambda)^2}{6} \left(\frac{\partial^4 V}{\partial \Phi \partial \Lambda^3}\right) \\ & - \frac{(\Delta_2 \Phi)^2(\Delta_2 \Lambda)^2}{36} \left(\frac{\partial^6 V}{\partial \Phi^3 \partial \Lambda^3}\right) - \dots \end{aligned}$$

Regarding the expressions for the $\Gamma_{\Phi \Lambda}$ component of the gravity gradient tensor in Eq. (31) of Fukushima (2018), the $+\frac{g_\Phi \tan \Phi}{R^2 \cos \Phi}$ term is wrong and should be corrected to the $+\frac{\tan \Phi}{R} g_\Lambda$ term. Equation (31) should be changed to:

$$\Gamma_{\Phi \Lambda} = \Gamma_{\Lambda \Phi} = \frac{1}{R^2 \cos \Phi} \left(\frac{\partial^2 V}{\partial \Phi \partial \Lambda}\right)_H + \frac{\tan \Phi}{R} g_\Lambda \quad (3)$$

Similarly, for the formula of the $\Gamma_{\Lambda H}$ component of the gravity gradient tensor in Fukushima (2018), the $-\frac{g_H}{R^2 \cos \Phi}$ term in Eq. (33) is wrong and should be changed to the $-\frac{g_\Lambda}{R}$

term. Then, Eq. (33) should be changed to:

$$\Gamma_{\Lambda H} = \Gamma_{H \Lambda} = \frac{1}{R \cos \Phi} \left(\frac{\partial^2 V}{\partial \Lambda \partial H}\right)_\Phi - \frac{g_\Lambda}{R} \quad (4)$$

where the expressions in Eqs. (31) and (33) belong to the incorrect derivation. The correct derivation of the formulas in Eqs. (3) and (4) is provided in ‘‘Appendix 1’’.

In the formula of the radial–radial component of the gravity gradient tensor Γ_{HH} of the spherical shell when the computation point is located inside the spherical shell ($H_B < H < H_T$) in Fukushima (2018), the $(4\pi G \rho / 3)(1 + 2R_B^3 / R^3)$ term in Eq. (48) should be replaced by $-(4\pi G \rho / 3)(1 + 2R_B^3 / R^3)$, i.e. the negative sign ‘-’ should be added, and it is a typo. Then, Eq. (48) should be changed to (Lin et al. 2020, Eq. (15c)):

$$\begin{aligned} & \Gamma_{HH, \text{analytical}} \\ &= \begin{cases} 0 & (H < H_B) \\ -(4\pi G \rho / 3)(1 + 2R_B^3 / R^3) & (H_B < H < H_T) \\ 2GM / R^3 & (H_T < H) \end{cases} \quad (5) \end{aligned}$$

Regarding the expression for the relative error of the second-order central difference formula in Eq. (77), the $-\left(\frac{f^{(4)}(t)}{12f''(t)}\right)(\Delta t)^2$ term should be changed to $\left(\frac{f^{(4)}(t)}{12f''(t)}\right)(\Delta t)^2$, i.e. the negative sign ‘-’ should be removed, and it is a typo. Then, Eq. (77) should be changed to:

$$\delta h_0(t) \equiv \frac{h_0(t) - f''(t)}{f''(t)} \approx \left(\frac{f^{(4)}(t)}{12f''(t)}\right)(\Delta t)^2 \quad (6)$$

3 Corrections to FORTRAN codes of Fukushima (2018)

The two FORTRAN subroutines `qgtess` and `qggtes` to calculate the gravitational acceleration vector (g_Φ and g_Λ) and gravity gradient tensor ($\Gamma_{\Phi\Phi}$, $\Gamma_{\Phi\Lambda}$, $\Gamma_{\Phi H}$, $\Gamma_{\Lambda\Lambda}$, $\Gamma_{\Lambda H}$, and Γ_{HH}) of the tesseroid in the code `xqtess.txt` in Tables 7–11 of the electronic supplementary material of Fukushima (2018) need to be revised in quadruple precision. The corrected subroutines `qgtess` and `qggtes` are presented in Tables 7–11 of this paper’s electronic supplementary material, where the revised parts are in bold fonts. The same parts in the code `xtess.txt` should be revised in double precision. Note that the FORTRAN function `vtess` is revised to `qvtess` in the subroutine `qggtes`, which is not in bold font. Based on the revised contents in Tables 7–11 of this paper’s electronic supplementary material, these revised codes will affect the evaluation of these components g_Φ , g_Λ , $\Gamma_{\Phi\Phi}$, $\Gamma_{\Phi\Lambda}$, $\Gamma_{\Phi H}$, $\Gamma_{\Lambda\Lambda}$, $\Gamma_{\Lambda H}$, and Γ_{HH} , where the calculation of the g_H will not be affected.

4 Numerical investigations

In this section, a simple numerical experiment is performed to reveal the magnitude of the error one makes when using the original codes of Fukushima (2018). The numerical experiment is carried out in a double-precision environment considering the computational efficiency, because quadruple precision generally requires more time than double precision. For instance, the ratio of quadruple precision to double precision is about $50.463/0.089 \approx 567$ per computation point with a single tesseroid on a desktop computer with an Intel i5-10400 CPU at 2.9 GHz and single-threaded operation in Sect. 5. Specifically, the values of the gravitational acceleration vector (g_ϕ and g_Λ) and gravity gradient tensor ($\Gamma_{\phi\phi}$, $\Gamma_{\phi\Lambda}$, $\Gamma_{\phi H}$, $\Gamma_{\Lambda\Lambda}$, $\Gamma_{\Lambda H}$, and Γ_{HH}) of a spherical shell are served as the analytical reference values for the calculated values of the discretized tesseroids forming the whole spherical shell with the original codes provided by Fukushima (2018) and revised codes.

Regarding the gravitational acceleration vector (g_ϕ and g_Λ) and gravity gradient tensor ($\Gamma_{\phi\Lambda}$, $\Gamma_{\phi H}$ and $\Gamma_{\Lambda H}$) of a spherical shell, their reference values are equal to zero. The three components of the gravity gradient tensor ($\Gamma_{\phi\phi}$, $\Gamma_{\Lambda\Lambda}$, and Γ_{HH}) satisfy Laplace’s equation outside the spherical shell and Poisson’s equation inside the spherical shell as MacMillan (1930), Kellogg (1967), Blakely (1995):

$$\Gamma_{\phi\phi,\text{analytical}} + \Gamma_{\Lambda\Lambda,\text{analytical}} + \Gamma_{HH,\text{analytical}} = 0 \quad (H < H_B \text{ or } H_T < H) \tag{7}$$

$$\Gamma_{\phi\phi,\text{analytical}} + \Gamma_{\Lambda\Lambda,\text{analytical}} + \Gamma_{HH,\text{analytical}} = -4\pi G\rho \quad (H_B < H < H_T) \tag{8}$$

When the computation point is located inside or outside the spherical shell, $\Gamma_{\phi\phi,\text{analytical}} = \Gamma_{\Lambda\Lambda,\text{analytical}}$ (Makhloof and Ilk 2008; Wild-Pfeiffer 2008). Substituting Eq. (5) into Eqs. (7) and (8) yields:

$$\Gamma_{\phi\phi,\text{analytical}} = \Gamma_{\Lambda\Lambda,\text{analytical}} = \begin{cases} 0 & (H < H_B) \\ (4\pi G\rho/3)(R_B^3/R^3 - 1) & (H_B < H < H_T) \\ -GM/R^3 & (H_T < H) \end{cases} \tag{9}$$

The detailed numerical settings are similar to those in Sect. 3.1 of Fukushima (2018). $G\rho = 1$ and the radius of the reference sphere is $R_0 = 6380$ km. The top and bottom heights of the spherical shell are $H_T = +10$ km and $H_B = -40$ km. The spherical latitude and longitude of the computation point are $\Phi = 0^\circ$ and $\Lambda = 180^\circ$. The height of the computation point varies from -100 to $+100$ km with an interval of 1 km. The error tolerance to calculate the gravitational potential is set as $\delta = 10^{-16}$ in double precision. The

computation points located on the surfaces of the spherical shell, i.e. $H = H_B$ or $H = H_T$, are shifted slightly inside the spherical shell as $H = (1 + \epsilon_D)H_B$ or $H = (1 - \epsilon_D)H_T$, where $\epsilon_D = 2^{-53} \approx 1.11 \times 10^{-16}$ is the double-precision machine epsilon (see Table 1 of Fukushima (2012)).

For other components g_ϕ , g_Λ , $\Gamma_{\phi\Lambda}$, $\Gamma_{\phi H}$, and $\Gamma_{\Lambda H}$, the absolute errors in \log_{10} scale are presented as:

$$\delta F = \log_{10} \left| \sum F \right| \tag{10}$$

where F means the g_ϕ , g_Λ , $\Gamma_{\phi\Lambda}$, $\Gamma_{\phi H}$, or $\Gamma_{\Lambda H}$. When the computation point is located below ($H < H_B$) the spherical shell for the components $\Gamma_{\phi\phi}$, $\Gamma_{\Lambda\Lambda}$, and Γ_{HH} , the absolute errors in \log_{10} scale are applied.

Regarding the components $\Gamma_{\phi\phi}$, $\Gamma_{\Lambda\Lambda}$, and Γ_{HH} when the computation point is located inside ($H_B < H < H_T$) and above ($H_T < H$) the spherical shell, their relative errors in \log_{10} scale are presented as:

$$\delta F = \log_{10} \left| \sum F/F_{\text{analytical}} - 1 \right| \tag{11}$$

where $F = \Gamma_{\phi\phi}$, $\Gamma_{\Lambda\Lambda}$, or Γ_{HH} . \sum means the sum of the calculated values of the discretized tesseroids forming the whole spherical shell. $F_{\text{analytical}}$ represents the analytical reference values of the spherical shell.

The absolute errors and relative errors in \log_{10} scale of the components g_ϕ , g_Λ , $\Gamma_{\phi\phi}$, $\Gamma_{\phi\Lambda}$, $\Gamma_{\phi H}$, $\Gamma_{\Lambda\Lambda}$, $\Gamma_{\Lambda H}$, and Γ_{HH} are shown in Fig. 1 using the revised FORTRAN codes and in Fig. 2 using the original FORTRAN codes provided by Fukushima (2018). The factors and units of the absolute errors of the gravitational acceleration vector (δg_ϕ and δg_Λ) and gravity gradient tensor ($\delta\Gamma_{\phi\phi}$, $\delta\Gamma_{\phi\Lambda}$, $\delta\Gamma_{\phi H}$, $\delta\Gamma_{\Lambda\Lambda}$, $\delta\Gamma_{\Lambda H}$, and $\delta\Gamma_{HH}$) are m^{-1} and m^{-2} , respectively. When evaluating the practical results of the gravitational acceleration vector and gravity gradient tensor using the original or revised FORTRAN codes, the term $G\rho R_0^2$ (i.e. the units of G , ρ , and R_0 are $\text{m}^3 \text{kg}^{-1} \text{s}^{-2}$, kg m^{-3} , and m) should be multiplied.

In Fig. 1a, the ranges of the absolute errors in \log_{10} scale of $\delta\Gamma_{\phi\phi}$, $\delta\Gamma_{\Lambda\Lambda}$, and $\delta\Gamma_{HH}$ are about $[-18, -14]$ in the interval of $[-100 \text{ km}, -40 \text{ km}]$ and the relative errors in \log_{10} scale are about $[-10, -6]$ in the interval of $[-40 \text{ km}, +100 \text{ km}]$. In any case, Fig. 1a approximately confirms the following equation:

$$|\delta F| \approx \log_{10} \left(\sqrt{\delta} \right) = \log_{10} \left(\sqrt{10^{-16}} \right) = -8 \tag{12}$$

excepting for the values of the $\delta\Gamma_{\phi\phi}$, $\delta\Gamma_{\Lambda\Lambda}$, and $\delta\Gamma_{HH}$ at $H_B = -40$ km and $H_T = +10$ km, i.e. the bottom and top boundaries of the spherical shell. In Eq. (12), $\delta F = \delta\Gamma_{\phi\phi}$, $\delta\Gamma_{\Lambda\Lambda}$, or $\delta\Gamma_{HH}$. The reason for this behavior in Eq. (12) is the error propagation when deriving higher-order gravitational field components by numerical differentiation of the

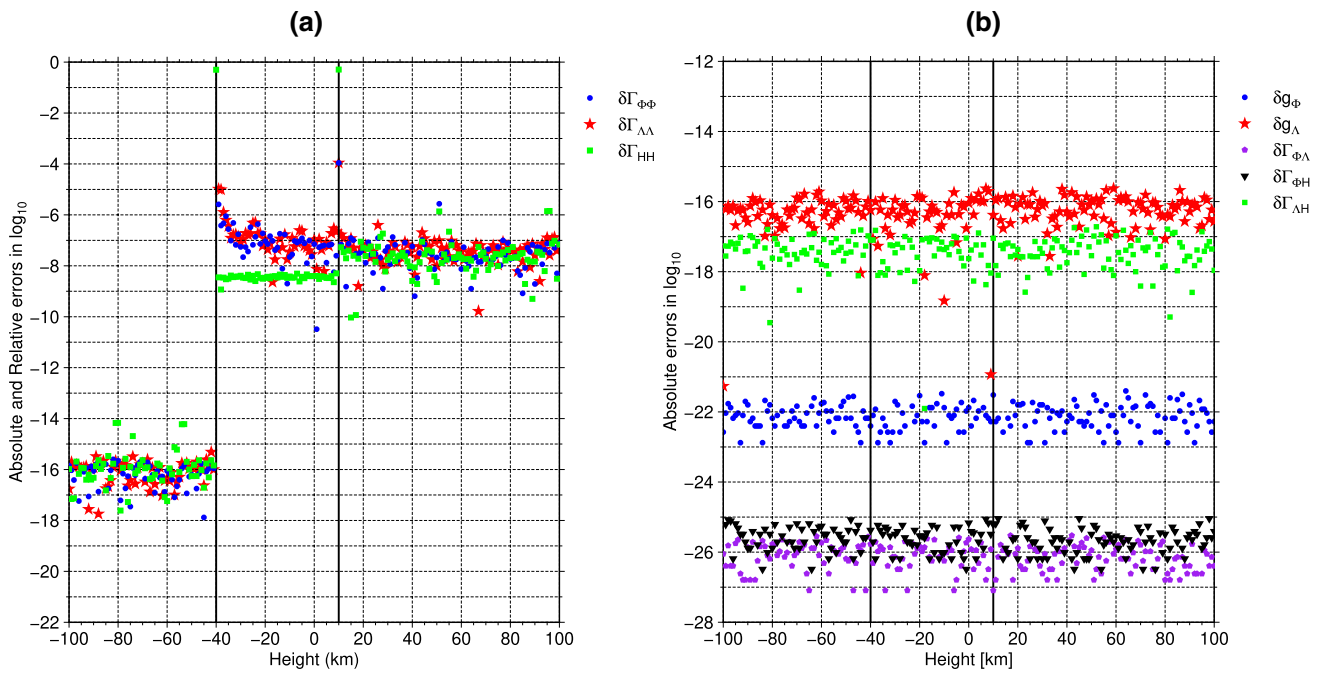


Fig. 1 **a** Illustration of the absolute errors and relative errors in \log_{10} scale of the $\delta\Gamma_{\phi\phi}$ with blue circle points, $\delta\Gamma_{\Lambda\Lambda}$ with red star points, and $\delta\Gamma_{HH}$ with green square points with the influence of the height H from -100 to $+100$ km with an interval of 1 km in double precision, where the absolute errors are in the range of $[-100$ km, -40 km] and the relative errors are in the range of $[-40$ km, $+100$ km]; **b** the absolute

errors in \log_{10} scale of the δg_{ϕ} with blue circle points, δg_{Λ} with red star points, $\delta\Gamma_{\phi\Lambda}$ with purple pentagon points, $\delta\Gamma_{\phi H}$ with black inverted triangle points, and $\delta\Gamma_{\Lambda H}$ with green square points. The two solid vertical lines at $H_B = -40$ km and $H_T = +10$ km mean the bottom and top boundaries of the spherical shell. These values are calculated using the revised codes

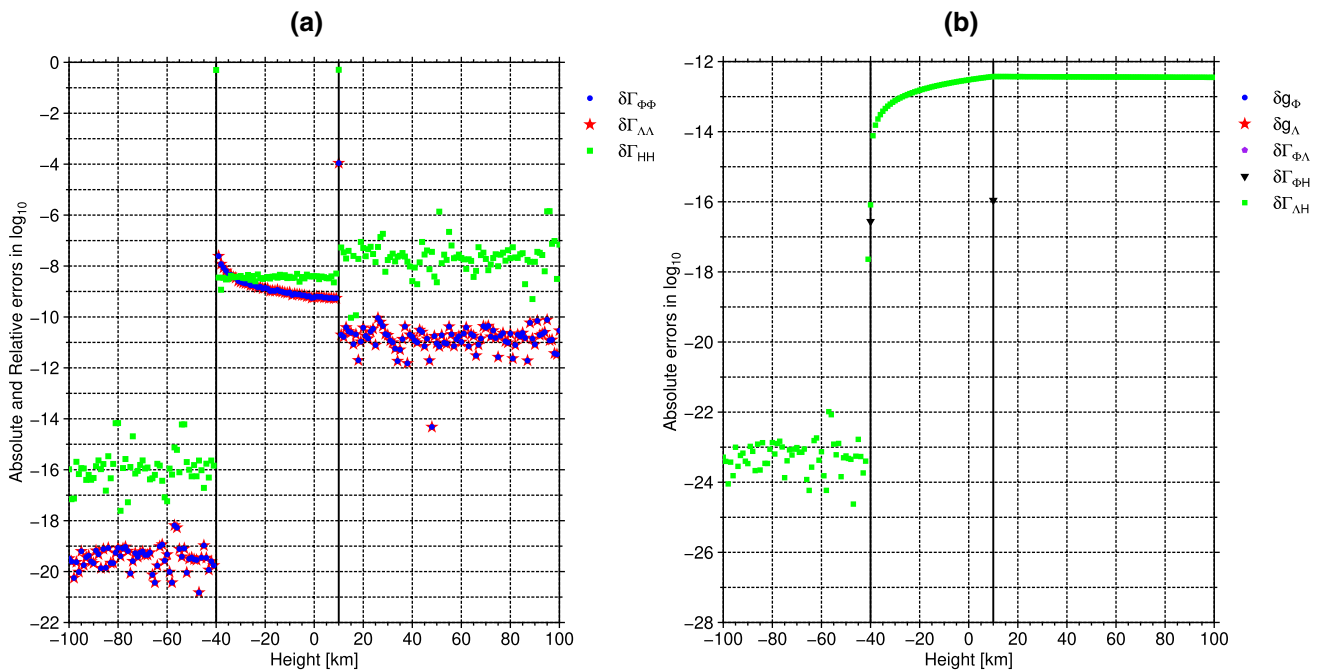


Fig. 2 Using the original codes provided by Fukushima (2018), other parameters are the same as in Fig. 1

gravitational potential. Specifically, the relative accuracy of the partially differentiated quantities is $\sqrt{\delta}$ for the gravity gradient tensor (Fukushima 2018), where δ is the error tolerance to compute the gravitational potential.

In Fig. 1b, the absolute errors in \log_{10} scale of the δg_ϕ , δg_Λ , $\delta \Gamma_{\phi\Lambda}$, $\delta \Gamma_{\phi H}$, and $\delta \Gamma_{\Lambda H}$ are mostly less than or equal to 10^{-16} , which are the random errors in double precision. Specifically, the ranges of the absolute errors in \log_{10} scale are about $[-23, -21]$ for the δg_ϕ , $[-21, -16]$ for the δg_Λ , $[-27, -25]$ for the $\delta \Gamma_{\phi\Lambda}$, $[-27, -25]$ for the $\delta \Gamma_{\phi H}$, and $[-22, -16]$ for the $\delta \Gamma_{\Lambda H}$.

By comparing the numerical results of Figs. 1a and 2a, it can be found that the absolute errors and relative errors in \log_{10} scale of the $\delta \Gamma_{HH}$ are almost the same with each other. In Fig. 2a, the ranges of the absolute errors in \log_{10} scale of the $\delta \Gamma_{\phi\phi}$ and $\delta \Gamma_{\Lambda\Lambda}$ are about $[-21, -18]$ in the range of $[-100 \text{ km}, -40 \text{ km}]$ and their relative errors in \log_{10} scale are about $[-14, -8]$ in the range of $[-40 \text{ km}, +100 \text{ km}]$. In Fig. 2b, the absolute errors in \log_{10} scale of the $\delta \Gamma_{\Lambda H}$ are in the ranges of $[-25, -22]$ in the interval of $[-100 \text{ km}, -40 \text{ km}]$ and $[-14, -12]$ in the interval of $[-40 \text{ km}, +100 \text{ km}]$. Regarding the absolute errors in \log_{10} scale of the δg_ϕ , δg_Λ , $\delta \Gamma_{\phi\Lambda}$, and $\delta \Gamma_{\phi H}$, there are no numerical values shown in Fig. 2b, excepting that the absolute errors of the $\delta \Gamma_{\phi H}$ are about -16 at $H_B = -40 \text{ km}$ and $H_T = +10 \text{ km}$.

Finally, numerical results reveal that the evaluation of the absolute errors and relative errors in \log_{10} scale of the $\delta \Gamma_{HH}$ does not be affected by using the original codes, because one of the conditional splits (i.e. if $\Phi_S \leq \Phi \leq \Phi_N$ and $\Lambda_W \leq \Lambda \leq \Lambda_E$ and either $H_B - \Delta_2 H < H < H_B$ or $H_T - \Delta_2 H < H < H_T$) in the revised code of the Γ_{HH} is not triggered. When using the original codes for the $\delta \Gamma_{\phi\phi}$ and $\delta \Gamma_{\Lambda\Lambda}$, their absolute and relative errors in \log_{10} scale were incorrectly improved by about 2–4 orders of magnitude. Regarding the $\delta \Gamma_{\Lambda H}$, the precision of its absolute errors in \log_{10} scale by using the original codes is erroneously improved by approximately 3–6 orders of magnitude in the range of $[-100 \text{ km}, -40 \text{ km}]$ and reduced by about 4–8 orders of magnitude in the range of $[-40 \text{ km}, +100 \text{ km}]$. The precision of the absolute errors in \log_{10} scale of the $\delta \Gamma_{\phi H}$ is reduced by about 9–11 orders of magnitude by using the original codes. Notably, the absolute errors in \log_{10} scale of the δg_ϕ , δg_Λ , $\delta \Gamma_{\phi\Lambda}$ and the majority of $\delta \Gamma_{\phi H}$ are not presented in Fig. 2b because of no numerical values. This is due to the fact that these values equal negative infinity. In other words, the calculated values of the δg_ϕ , δg_Λ , $\delta \Gamma_{\phi\Lambda}$ and the most of $\delta \Gamma_{\phi H}$ when using the original codes in Fukushima (2018) are equal to zero and their absolute errors in \log_{10} scale are $\log_{10} 0 = -\infty$.

5 Computer programs of the xtess.f90 and xqtess.f90

To make better use of the revised FORTRAN codes, the xtess.f90 and xqtess.f90 are presented at the GitHub website <https://github.com/xiaoledeng/xtess-xqtess>. The total CPU time of the xtess.f90 and xqtess.f90 to calculate all 10 components of the V , g_ϕ , g_Λ , g_H , $\Gamma_{\phi\phi}$, $\Gamma_{\phi\Lambda}$, $\Gamma_{\phi H}$, $\Gamma_{\Lambda\Lambda}$, $\Gamma_{\Lambda H}$, and Γ_{HH} is $3.568/40 \text{ s} \approx 0.089 \text{ s}$ per computation point when $\delta = 10^{-16}$ in double precision and 50.463 s per computation point when $\delta = 10^{-33}$ in quadrature precision with a single tesseroid mass body. These values are obtained on a desktop computer with an Intel i5-10400 CPU at 2.9 GHz using the single-threaded operation.

When applying the gravitational potential, gravitational acceleration vector, and gravity gradient tensor using these FORTRAN codes in the practical applications, the term $G\rho R_0^2$ should be multiplied with the output numerical values to obtain the units $\text{m}^2 \text{s}^{-2}$ for the gravitational potential, m s^{-2} for the gravitational acceleration vector, and s^{-2} for the gravity gradient tensor, where the units of G , ρ , and R_0 are $\text{m}^3 \text{kg}^{-1} \text{s}^{-2}$, kg m^{-3} , and m , respectively.

6 Conclusions and consequences for Fukushima (2018)

Theoretically, the revised parts in the original codes xtess.txt and xqtess.txt have impacts on the calculation of these components of the gravitational acceleration vector (i.e. g_ϕ and g_Λ) and gravity gradient tensor (i.e. $\Gamma_{\phi\phi}$, $\Gamma_{\phi\Lambda}$, $\Gamma_{\phi H}$, $\Gamma_{\Lambda\Lambda}$, $\Gamma_{\Lambda H}$, and Γ_{HH}). Regarding the Γ_{HH} , the influence on the calculation results only occurs when one of the conditional splits (i.e. if $\Phi_S \leq \Phi \leq \Phi_N$ and $\Lambda_W \leq \Lambda \leq \Lambda_E$ and either $H_B - \Delta_2 H < H < H_B$ or $H_T - \Delta_2 H < H < H_T$) is performed. The evaluation of the gravitational potential V and the radial component of the gravitational acceleration vector g_H in the original codes xtess.txt and xqtess.txt will not be affected.

Numerical results reveal that the absolute errors obtained by using the corrected codes are at a lower precision level by 2–4 orders of magnitude for the $\delta \Gamma_{\phi\phi}$ and $\delta \Gamma_{\Lambda\Lambda}$ components of the gravity gradient tensor. Regarding the $\delta \Gamma_{\Lambda H}$ component of the gravity gradient tensor, the precision level of the absolute errors by using the corrected codes is reduced by 3–6 orders of magnitude when the computation point is located below the spherical shell and improved by 4–8 orders of magnitude when the computation point is located in and above the spherical shell. When the computation point is located on the bottom and top boundaries of the spherical shell, the precision level of the absolute errors for the $\delta \Gamma_{\phi H}$ component of the gravity gradient tensor by using the corrected codes is improved by 9–11 orders of magnitude. If

using the original codes for the g_ϕ and g_Λ components of the gravitational acceleration vector and the $\delta\Gamma_{\phi\Lambda}$ and most of the $\delta\Gamma_{\phi H}$ components of the gravity gradient tensor, their calculated values of the tesseroids are equal to zero. When using the revised codes for these components, their absolute errors in \log_{10} scale are in ranges of about $[-23, -21]$ for the δg_ϕ , $[-21, -16]$ for the δg_Λ , $[-27, -25]$ for the $\delta\Gamma_{\phi\Lambda}$, and $[-27, -25]$ for the $\delta\Gamma_{\phi H}$.

The previous study that quoted the original FORTRAN codes provided by Fukushima (2018) to calculate the gravitational field of a tesseroid should be carefully considered based on the above potential impacts. For example, Lin et al. (2020) calculated the gravitational potential V , radial component V_z of the gravitational acceleration vector, and radial–radial component V_{zz} of the gravity gradient tensor in Sect. 3.7 based on the use of the original FORTRAN codes in Fukushima (2018). Fortunately, these three components V , V_z , and V_{zz} are not affected, although the FORTRAN code of the V_{zz} needs to be modified, whereas in Sect. 4.2 gravitational acceleration vector of tesseroid, Sect. 4.3 gravity gradient tensor of tesseroid, Sect. 4.4 polar tesseroid, and Sect. 4.5 polar cap slab of the electronic supplement material of Fukushima (2018), the evaluation of the gravity field quantities (e.g. the total gravitational acceleration $g = \sqrt{g_\phi^2 + g_\Lambda^2 + g_H^2}$, magnitude of the vector representing the deflection of the vertical referred to the normal vector of the reference sphere $\theta = \tan^{-1}\left(\frac{\sqrt{g_\phi^2 + g_\Lambda^2}}{g_H}\right)$, azimuthal angle of the vector representing the deflection of the vertical $A = \tan^{-1}(g_\phi/g_\Lambda)$, $\Delta A = \tan^{-1}\left(\frac{(\phi_C - \phi)g_\Lambda - (\Lambda_C - \Lambda)g_\phi}{(\phi_C - \phi)g_\phi + (\Lambda_C - \Lambda)g_\Lambda}\right)$, and these components $\Gamma_{\phi\phi}$, $\Gamma_{\phi\Lambda}$, $\Gamma_{\phi H}$, $\Gamma_{\Lambda\Lambda}$, and $\Gamma_{\Lambda H}$ of the gravity gradient tensor) may be wrong and needs to be carefully investigated especially when these components of the gravitational acceleration vector (i.e. g_ϕ and g_Λ) and gravity gradient tensor (i.e. $\Gamma_{\phi\phi}$, $\Gamma_{\phi\Lambda}$, $\Gamma_{\phi H}$, $\Gamma_{\Lambda\Lambda}$, and $\Gamma_{\Lambda H}$) are included.

Regarding the impacts of replacing the revised codes in this study with the original codes in Fukushima (2018) when considering practical applications for modeling the gravitational signals of mass distributions of the Earth or other planetary bodies, further empirical research is required to explore these in the future.

Supplementary Information The online version contains supplementary material available at <https://doi.org/10.1007/s00190-022-01673-2>.

Acknowledgements We are very grateful to Editor-in-Chief Prof. J. Kusche, associate editor, and two anonymous reviewers for their valuable comments and suggestions, which greatly improved the manuscript. This study is supported by the Alexander von Humboldt Foundation in Germany.

Funding Open Access funding enabled and organized by Projekt DEAL.

Data availability The codes that support the findings of this study are openly available at the GitHub website <https://github.com/xiaoledeng/xtess-xqtess>.

Declarations

Conflict of Interest The author declares no competing financial interests.

Open Access This article is licensed under a Creative Commons Attribution 4.0 International License, which permits use, sharing, adaptation, distribution and reproduction in any medium or format, as long as you give appropriate credit to the original author(s) and the source, provide a link to the Creative Commons licence, and indicate if changes were made. The images or other third party material in this article are included in the article’s Creative Commons licence, unless indicated otherwise in a credit line to the material. If material is not included in the article’s Creative Commons licence and your intended use is not permitted by statutory regulation or exceeds the permitted use, you will need to obtain permission directly from the copyright holder. To view a copy of this licence, visit <http://creativecommons.org/licenses/by/4.0/>.

Appendix 1: Derivation of the $\Gamma_{\phi\Lambda}$ and $\Gamma_{\Lambda H}$ components of the gravity gradient tensor

In this part, the detailed derivation of the $\Gamma_{\phi\Lambda}$ and $\Gamma_{\Lambda H}$ components of the gravity gradient tensor is presented to confirm the correctness of the formulas of the $\Gamma_{\phi\Lambda}$ and $\Gamma_{\Lambda H}$ in Eqs. (3) and (4).

Based on Eqs. (6) and (38) of Casotto and Fantino (2009), the general formula of the gravitational acceleration vector is obtained as:

$$V_{,p}^* = \frac{1}{h_p} \frac{\partial V}{\partial u^p} \tag{13}$$

$$h_1 = R \cos \Phi, \quad h_2 = R, \quad h_3 = 1 \tag{14}$$

where $p = 1, 2, 3$. $u^1 = \Lambda$, $u^2 = \Phi$, and $u^3 = R$ are the spherical longitude, latitude, and geocentric distance of the computation point. V is the gravitational potential and $\frac{\partial V}{\partial u^p}$ are its first-order derivatives. Note that $u^3 = R$ is denoted as H in Fukushima (2018).

The g_Λ component of the gravitational acceleration vector is obtained with $p = 1$ in Eq. (13) as:

$$g_\Lambda = V_{,1}^* = \frac{1}{R \cos \Phi} \frac{\partial V}{\partial \Lambda} \tag{15}$$

Combining Eqs. (13) and (14) of Casotto and Fantino (2009) yields the general formula of the gravity gradient tensor as:

$$\begin{aligned}
 V_{:pq}^* &= \frac{1}{h_p h_q} \left(\frac{\partial^2 V}{\partial u^p \partial u^q} - \Gamma_{qp}^s \frac{\partial V}{\partial u^s} \right) \\
 &= \frac{1}{h_p h_q} \left(\frac{\partial^2 V}{\partial u^p \partial u^q} - \sum_{s=1}^3 \Gamma_{qp}^s \frac{\partial V}{\partial u^s} \right)
 \end{aligned}
 \tag{16}$$

where $p, q, s = 1, 2, 3$. Note that the Einstein summation convention has been applied in Eq. (16). Γ_{qp}^s is the Christoffel's symbol of the second kind, which can be referred to in Eqs. (39)–(41) of Casotto and Fantino (2009) and Table 2 of Deng and Ran (2021).

The $\Gamma_{\Phi\Lambda}$ component of the gravity gradient tensor is obtained with $p = 2$ and $q = 1$ in Eq. (16) as:

$$\begin{aligned}
 \Gamma_{\Phi\Lambda} &= V_{:21}^* = \frac{1}{h_2 h_1} \left[\frac{\partial^2 V}{\partial u^2 \partial u^1} \right. \\
 &\quad \left. - \left(\Gamma_{12}^1 \frac{\partial V}{\partial u^1} + \Gamma_{12}^2 \frac{\partial V}{\partial u^2} + \Gamma_{12}^3 \frac{\partial V}{\partial u^3} \right) \right] \\
 &= \frac{1}{R^2 \cos \Phi} \left(\frac{\partial^2 V}{\partial \Phi \partial \Lambda} + \tan \Phi \frac{\partial V}{\partial \Lambda} \right) \\
 &= \frac{1}{R^2 \cos \Phi} \left(\frac{\partial^2 V}{\partial \Phi \partial \Lambda} \right) + \frac{\tan \Phi}{R} g_\Lambda
 \end{aligned}
 \tag{17}$$

where $\Gamma_{12}^1 = -\tan \Phi$ and $\Gamma_{12}^2 = \Gamma_{12}^3 = 0$ are referred to in Table 2 of Deng and Ran (2021). The equation $\frac{1}{R \cos \Phi} \frac{\partial V}{\partial \Lambda} = g_\Lambda$ in Eq. (15) is applied. Similarly, the expression for the $\Gamma_{\Lambda\Phi}$ can be obtained with $p = 1$ and $q = 2$ in Eq. (16) and is the same as the $\Gamma_{\Phi\Lambda}$.

Furthermore, the $\Gamma_{\Lambda H}$ component of the gravity gradient tensor is obtained with $p = 1$ and $q = 3$ in Eq. (16) as:

$$\begin{aligned}
 \Gamma_{\Lambda H} &= V_{:13}^* = \frac{1}{h_1 h_3} \left[\frac{\partial^2 V}{\partial u^1 \partial u^3} \right. \\
 &\quad \left. - \left(\Gamma_{31}^1 \frac{\partial V}{\partial u^1} + \Gamma_{31}^2 \frac{\partial V}{\partial u^2} + \Gamma_{31}^3 \frac{\partial V}{\partial u^3} \right) \right] \\
 &= \frac{1}{R \cos \Phi} \left(\frac{\partial^2 V}{\partial \Lambda \partial H} - \frac{1}{R} \frac{\partial V}{\partial \Lambda} \right) \\
 &= \frac{1}{R \cos \Phi} \left(\frac{\partial^2 V}{\partial \Lambda \partial H} \right) - \frac{g_\Lambda}{R}
 \end{aligned}
 \tag{18}$$

where $\Gamma_{31}^1 = 1/R$ and $\Gamma_{31}^2 = \Gamma_{31}^3 = 0$ are referred to in Table 2 of Deng and Ran (2021). The equation $\frac{1}{R \cos \Phi} \frac{\partial V}{\partial \Lambda} = g_\Lambda$ in Eq. (15) is applied. Analogously, the expression for the $\Gamma_{H\Lambda}$ can be obtained with $p = 3$ and $q = 1$ in Eq. (16) and is the same as the $\Gamma_{\Lambda H}$.

Note that when the subscripts H and Φ are added for the first terms in Eqs. (17) and (18), Eqs. (17) and (18) are the same as Eqs. (3) and (4).

References

Blakely RJ (1995) Potential theory in gravity and magnetic applications. Cambridge University Press, Cambridge. <https://doi.org/10.1017/CBO9780511549816>

Casotto S, Fantino E (2009) Gravitational gradients by tensor analysis with application to spherical coordinates. *J Geod* 83(7):621–634. <https://doi.org/10.1007/s00190-008-0276-z>

Deng XL, Ran J (2021) Higher-order gravitational potential gradients by tensor analysis in spherical coordinates. *J Geod* 95(7):1–13. <https://doi.org/10.1007/s00190-021-01539-z>

Fukushima T (2012) Numerical computation of spherical harmonics of arbitrary degree and order by extending exponent of floating point numbers. *J Geod* 86(4):271–285. <https://doi.org/10.1007/s00190-011-0519-2>

Fukushima T (2018) Accurate computation of gravitational field of a tesseroid. *J Geod* 92(12):1371–1386. <https://doi.org/10.1007/s00190-018-1126-2>

Kellogg O (1967) Foundations of potential theory. Springer, Berlin. <https://doi.org/10.1007/978-3-642-86748-4>

Lin M, Denker H, Müller J (2020) Gravity field modeling using tesseroids with variable density in the vertical direction. *Surv Geophys* 41(4):723–765. <https://doi.org/10.1007/s10712-020-09585-6>

MacMillan WD (1930) The theory of the potential. Dover, New York

Makhloof AA, Ilk KH (2008) Effects of topographic–isostatic masses on gravitational functionals at the earth’s surface and at airborne and satellite altitudes. *J Geod* 82(2):93–111. <https://doi.org/10.1007/s00190-007-0159-8>

Wild-Pfeiffer F (2008) A comparison of different mass elements for use in gravity gradiometry. *J Geod* 82(10):637–653. <https://doi.org/10.1007/s00190-008-0219-8>